Electronics and Computer Science
Faculty of Physical Sciences and Engineering
University of Southampton

Implementation of The Subsample Volume Doppler Algorithm within BrainTV

Jakub Markiewicz

Supervisor: Dr Andrea Lecchini Visintini

December 5, 2023

A project progress report submitted for the award of:
Electrical and Electronic Engineering (BEng)

1. Project Description

Measuring Brain Tissue Pulsations (BTPs) with ultrasound is a relatively unexplored field. Furthermore, many algorithms have been proposed to estimate the Doppler velocity, which provides crucial insight into analyzing blood flow patterns in the brain by processing the phase shift of echo signals. One approach is named 'The Subsample Volume Doppler' (SDopp) algorithm (Hoeks et al. 1994) [1]. This algorithm is implemented in the novel graphical user interface (GUI): BrainTV.

BrainTV is a software used to analyse the ultrasound signal and extract features, such as CO2 levels, blood pressure, and the aforementioned Doppler velocity. Currently, the connection between the biophysics of ultrasound and the implementation of the SDopp algorithm within the software is not well documented. There also exist several problems with obtaining reliable results via medical ultrasound, such as the effect of artefacts and noise at deeper depths; data is often discarded or unreliable and hence clinical applications are not yet fully realized.

This project aims to be a clear overview of The Subsample Volume Doppler algorithm and its implementation. The paper will generally discuss the signal processing that is involved in obtaining the phase shift, as well as serve to be a detailed documentation of the code structure, data flow, and parameters involved. In addition, the limitations of the algorithm will also be noted and, if time permits, be addressed and improved upon. These improvements will aim to reduce the rate at which data is discarded. Future research may be done to continue this last goal.

2. Literature Review and Background Research

2.1. Introduction

This chapter aims to provide a comprehensive review of the key concepts in medical ultrasound in relation to acquiring BTP data. Emphasis will be put on the significance that the Doppler velocity has on analysing blood flow in the brain and hence contextualize such algorithms as the subsample approach. There will be two main sections, the Physics of Ultrasound, and Signal Processing, where each topic will be discussed in detail. To conclude, attention will be brought to current research gaps and challenges in literature.

2.2. Physics of Ultrasound

2.2.1. Key Concepts

Ultrasound is a high frequency sound wave used to image the body and brain non-invasively. It can provide insight into moving structures, such as tissues or blood flow in vessels [2]. Frequency of ultrasound is typically 2-10MHz, where higher frequencies (5-10MHz) are more commonly used in high resolution recordings of tissues and vessels. However, this range results in less penetration in soft tissues due to attenuation. Ultrasound relies on the emitted signal being reflected as an echo, back to the same probe (transducer). The level of reflection is dependent on the difference of acoustic impedance in two mediums. Acoustic impedance can be approximated as the product of density with the velocity of the sound wave through the particular medium

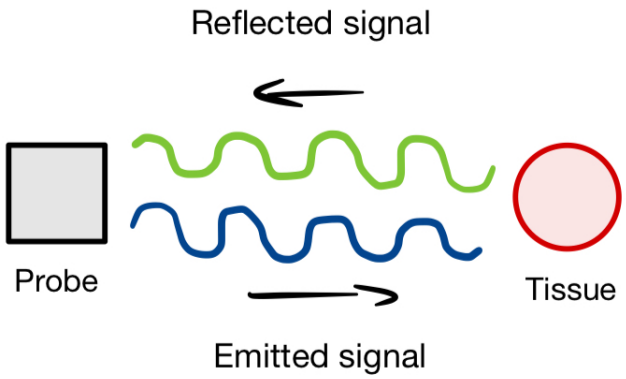

Figure 1: Probe is both the emitter and receiver

[3]. At large differences (air and bone), almost all of the energy of the sound wave is reflected back. Therefore, it is more common to use ultrasound for imaging soft tissues such as the brain. Although this is one example where attenuation is useful, there are other forms which can produce artefacts. Attenuation produces energy losses through reflection, refraction, scattering and absorption. Absorption occurs due to the friction between oscillating particles and is the largest cause of energy loss, in the form of heat. In the context of BTP data collection, high frequency ultrasound results in high absorption, and moreover unreliable measurements at deeper depths. It is common to observe noise and artefacts at deeper gates.

2.2.2. Brain Tissue Pulsation (BTP) Scanning

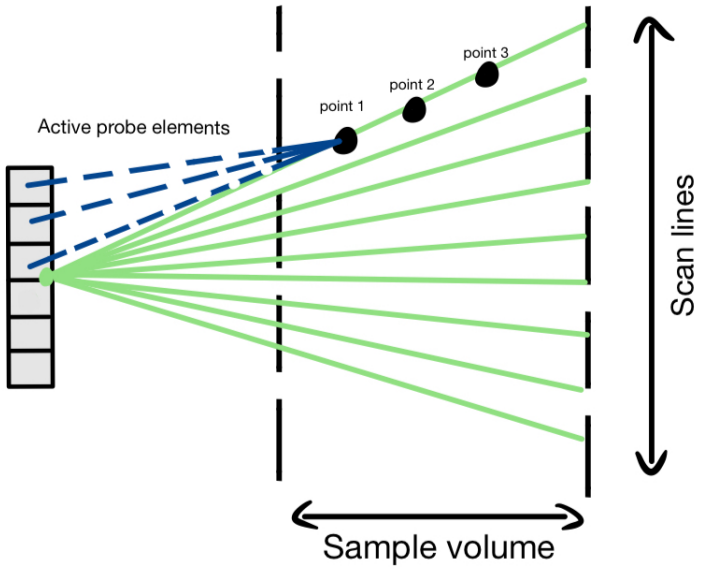

Figure 2: Tissue scanning

On the other hand, BTP measurements can be effectively made at smaller depths. The user may select the area of interest, known as a sample volume or 'gate'. The probe is activated by briefly passing a current, to which its elements emit a pulse towards a tissue, in the form of a point on a scan line [4]. The pulse is reflected as it travels to the focal

point, back to the probe. Once all the waves return, the current is passed again to transmit new sound waves towards a new point along the scan line. This is an iterative process as shown in figure 2. Once all the points along the scan line are measured, a new scan line is selected and the process continues.

2.2.3. Pulse Wave (PW) Doppler

Using a PW system, a sample volume may be interrogated by measuring the relative time difference of the reflected signals. This is analogous to having the phase shift. Consequently, it is possible to then estimate the Doppler velocity, which is proportional to the change in phase shift of the signal at that particular gate/depth:

$$v(m,n) = \frac{\lambda_n}{2}\left(\frac{\phi(m,n) - \phi(m,n-1)}{2\pi T}\right) \tag{1}$$

where $\phi(m,n)$ is the phase of the signal returned from m^{th} depth and n^{th} pulse. λ_n is the Nyquist sampling rate, and T is the reciprocal of the pulse repetition frequency (PRF). An important quality of PW systems is the required delay time when awaiting on the reflected signal. PRF refers to the number of pulses sent over a period of one second, which requires some consideration of the motion velocity of the tissue of interest. The ratio between emission and waiting time is around 0.1% to 99.9%, which implies a maximum limit to the PRF at which, beyond, the echoes from the gate no longer have enough time to return before the next pulses are emitted [5]. This is an example of an aliasing artefact.

The autocorrelation estimator developed by Kasai et al. (1985) [6], is the most commonly used function for this velocity estimation. It computes the mean velocity of the reflected signals within a single sample volume over a series of pulse cycles:

$$v(m,n) = \frac{\lambda_n}{4\pi T} arg\left\{\sum_{b=2-PL}^{0} S'(m,n-b)S'^{*}(m,n-b-1)\right\} \tag{2}$$

where PL is the package length, or the number of pulses the mean velocity is estimated over. $S'^{*}(m,n)$ refers to the received signal after demodulation, the details of which is shown in the next section.

The sampling volume has to be carefully selected to accommodate for tissue movements. If the tissue moves significantly during the recordings, the enclosed volume will change and the estimate of the velocity will be inaccurate.

2.3. Signal Processing

2.3.1. Quadrature Demodulation

The first step in processing an RF (radio frequency; ultrasound) signal is converting from a real to a complex signal. This is done via quadrature demodulation. There are two signals used for demodulation, the inphase D_I signal and the quadrature D_Q signal. Both share the same center frequency, w_c, as the RF signal; the quadrature signal is shifted by $\frac{\pi}{2}$ relative to the inphase signal. The following equations show the process of demodulation mathematically [7].

It is common to represent an RF signal at the receiver as:

$$\begin{aligned} S(t) &= A(t)cos(w_c t + \phi(t)) \\ &= A(t)cos(w_c t)cos[\phi(t)] - A(t)sin(w_c t)sin[\phi(t)] \end{aligned} \tag{3}$$

where $A(t)$ is the amplitude and $\phi(t)$ is the phase at a given time. In order to extract information from the signal, it must be demodulated. For this we require an inphase D_I and a quadrature Q_I signal:

$$D_I(t) = cos(w_c t) \tag{4}$$

$$D_Q(t) = sin(w_c t) \tag{5}$$

Multiplying the RF signal by the inphase demodulating signal gives:

$$S(t)D_I(t) = \frac{1}{2}A(t)\{cos(2w_c t + \phi(t)) + cos[\phi(t)]\} \tag{6}$$

Multiplying the RF signal by the quadrature demodulating signal gives:

$$S(t)D_Q(t) = \frac{1}{2}A(t)\{sin(2w_c t + \phi(t)) - sin[\phi(t)]\} \tag{7}$$

By applying a low pass filter (LPF) with a cutoff frequency at $\leq w_c$, all the terms with $2w_c$ are removed. As a result, this yields the respective inphase (real) and quadrature (imaginary) components of the complex signal:

$$I(t) = \frac{K}{2}A(t)cos[\phi(t)] \tag{8}$$

$$Q(t) = -\frac{K}{2}A(t)sin[\phi(t)] \tag{9}$$

where K is the gain due to LPF. Therefore, the complex signal is:

$$\begin{aligned} S'(t) &= I(t) + jQ(t) \\ &= A(t)e^{-j\phi(t)} \end{aligned} \tag{10}$$

Obtaining the complex IQ signal from a reflected RF pulse is crucial in extracting features such as the phase and envelope. This is best shown by an IQ graph in figure 3. Consequently, the phase can be expressed as:

$$-\phi(t) = \arctan\left(\frac{Q(t)}{I(t)}\right) \tag{11}$$

The envelope may also be extracted by taking the absolute value of the IQ vector:

$$E = \sqrt{I(t)^2 + Q(t)^2} = \frac{K}{2}A(t) \tag{12}$$

2.3.2. Subsample Volume Processing (SDopp Algorithm)

Pairs of IQ signals are, in most velocity estimators (e.g. Autocorrelation function; Kasai et al. 1985), used as the single sample volume over which the mean is calculated.

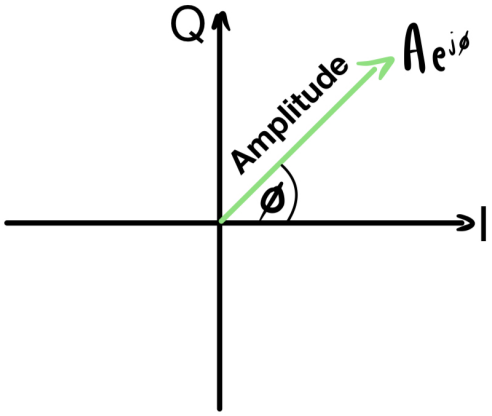

Figure 3: IQ vector

Equation 11 expresses one RF signal at the receiver after demodulation. However, because the goal is calculating the phase shift, it is important to account for multiple RF signals as well as the digitization process. Moreover, the complex IQ signal is better expressed as:

$$S'(m,n) = A(m,n)e^{-j\phi(m,n)} \tag{13}$$

where parameters m and n are introduced to index the signal by depth and pulse number respectively.

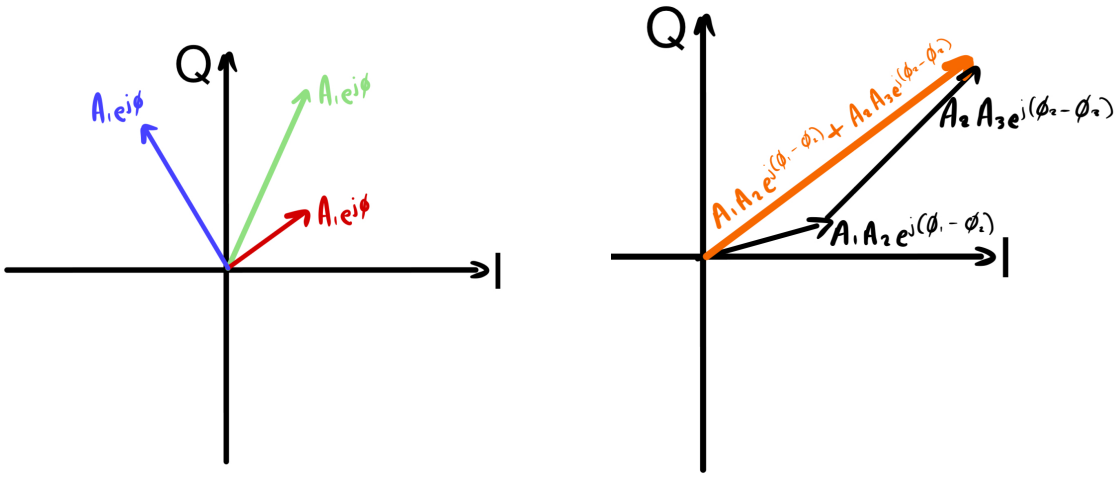

((a)) ((b))

Figure 4: Process of autocorrelation function on three IQ samples. The summed vector represents the mean phase shift, from which the velocity is estimated.

A major assumption of most PW systems is that the phase of the received echo changes linearly with depth, though the spatial distribution of reflected pulses suggests this is not the case (Hoeks et al. 1994). The result of using PW systems with this assumption is the present variance in measured velocities. The solution to this is to split the observation window into smaller 'subsample' volumes and then find the mean velocity using the sum of these subsamples. This can be shown mathematically by the estimator developed by Hoeks et al. (1994); also known as The Subsample Volume Doppler (SDopp) algorithm:

$$v(m,n) = \frac{\lambda_n}{4\pi T} arg\left\{ \sum_{a=2-ND}^{0} \sum_{b=2-PL}^{0} S'(m-a,n-b)S'^{*}(m-a,n-b-1) \right\} \tag{14}$$

where ND is the number of subsamples over which the velocity is estimated.
Consequently, when a single depth is used, SDopp reduces to the autocorrelation function. This method of estimation reduces the variance in velocity.

2.4. Challenges in Literature

Despite advancements being made in the field of medical ultrasound for collecting BTP data, there nevertheless exist many challenges yet to be addressed by future research. In this section, the most common problems are discussed.

2.4.1. Attenuation, Artefacts and Noise

In the study by Turner et al. (2020) [8], the researchers had to discard 5% of the BTP data due to artefacts in the form of motion (coughing, blinking, probe movement) and noise at deeper depths (82-86mm). Although this seems like a relatively low discard rate, there are implied concerns regarding standardization and replicability of the data collection methodology. The lack of standardization and mitigation strategies to tackle artefacts prevents the development of clinical diagnostic applications, particularly at deeper gates. Future research must be done to aid validate the current findings and techniques, possibly through direct replication. Researchers have a responsibility to clearly list their equipment apparatus to make this accessible.

Attenuation in general is a topic of debate in literature. Some researchers highlight the benefits of avoiding reflections at undesired depths by considering acoustic impedance, which is useful in probe fabrication [9]. In contrast, some studies report on the importance of achieving high resolution with the trade off with high absorption. Exploring the impact of attenuation on pulse wave systems should be essential.

2.4.2. Biased Samples, Extraneous Variables, and Ethics

In the study by Ince et al. (2020) [10], the researchers perform a systematic review of 10 BTP papers. Most studies currently claim to only sample healthy volunteers. A lack of standardization of the sampling process raises ethical concerns, particularly what makes a healthy 'sample'. Researchers must be transparent and report their procedures to ensure integrity of this novel research and ensure replicability of this sampling process.

There is also a lack of consideration in terms of extraneous variables such as undiagnosed medical conditions or the apparatus used. It is important to account for confounding factors to ensure reliability of their results. Furthermore, emphasis must be put on the level of training of the operator during data collection, as well as making training standardized to ensure consistent data collection and replicability of results.

3. Work Completed to Date

3.1. Understanding the Algorithm

Understanding the SDopp estimator has been the primary focus. To achieve this, a repository was created in GoodNotes and OneDrive to collect relevant studies for reading,

highlighting and future referencing. The study by Hoeks et al. (1994) was the first paper analysed, for it contains the relevant algorithm. Without previous knowledge in medical ultrasound, reading this paper proved difficult.

Further resources in the physics of ultrasound (Powles et al. 2018) and signal processing for medical imaging (Ali et al. 2008), were read to solve this problem. These studies were highlighted in GoodNotes, and summarised in brief written notes. Returning to the original SDopp paper, the background knowledge allowed a greater understanding of the algorithm.

3.2. BrainTV GUI

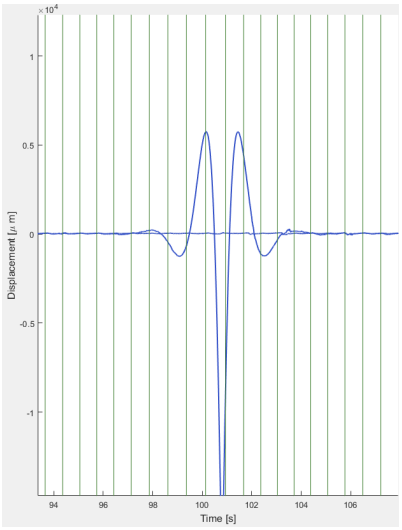

((a)) Displacement in gates 24 and 25. Artefact in gate 24.

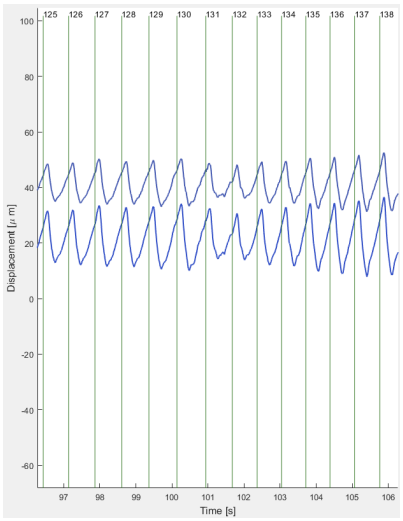

((b)) Displacement in gates 8 and 9. No artefacts present.

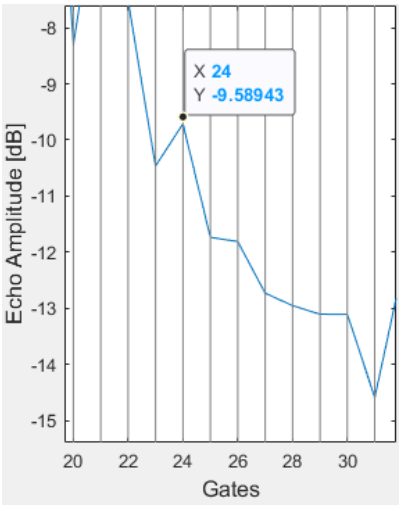

((c)) Echo amplitude at gate 24; -9.59dB

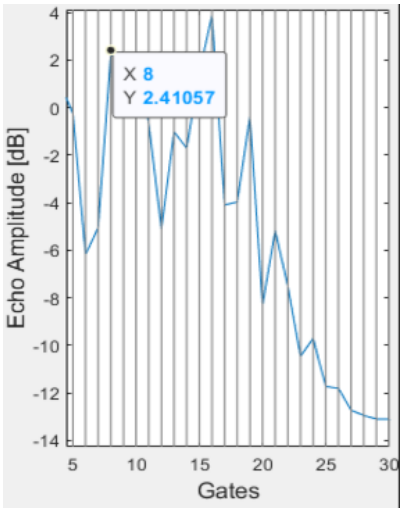

((d)) Echo amplitude at gate 8; +2.41dB

Figure 5: Subfigures 5(a) and 5(b) show the relation between deeper gates and the presence of artefacts. In subfigure 5(a) the amplitude remains at 0μm until large phase shift between 100-102seconds. Both signals have to be discarded. Subfigures 5(c) and 5(d) show no relation between artefacts and the echo amplitude; the reflected signal should have a lower energy and yet gate 8 (no artefacts present) shows a gain. The effect of the LPF and noise could explain this.

Some time was dedicated to learning the BrainTV GUI; running both the MATLAB and Python version. The python version is a translation of the MATLAB version. To achieve this, the provided user guide was read in detail. In both versions, the same tasks were tested: importing data, extracting features, zooming, exporting to an .xlsx excel file.

Despite being more proficient in python, it was obvious early on that the MATLAB version was superior to the Python version, due to less random crashes.

3.3. Data Format and Code Implementation

Choosing to focus on the MATLAB version meant that some time was given to becoming proficient enough in the language to be able to understand the BrainTV code.

The algorithm file VSDopp_v2_BrainTV.m was initially looked at, which contains the implementation of the VSDopp estimator. It has been a difficult process to decipher how exactly the algorithm in the Hoeks et al. (1994) paper translates to code until recently; the programmer used a different representation of the algorithm (shown in the Ph.D Thesis by J. Kucewicz, 2004). The lack of comments caused this delay. Progress has been made to address this.

```
41  %b is 0, a is [-2,-1,0]
42  b = 2 - PL:1:0;
43  a = 2 - ND:1:0;
44
45  %Creates a matrix array for storing values, hence all zeroed.
46  %Matrix with length of av_data cell e.g. 4 rows, and 3 columns (length of
47  %a).
48  VD = zeros(length(av_data)-2,length(a));
49
50  %Matrix with length of av_data cell rows and 2 columns.
51  v = zeros(length(av_data)-2,2);
52
53  %Matrix with length of av_data cell rows and mm (no. of gates) columns.
54  V_dop = zeros(length(av_data)-2,mm);
55
56  %for loop is on until n = length(av_data)-2
57  %e.g. if length is 4, then n = 1, then n = 2. (4-2 = 2)
58  for n = 1:length(av_data)-2
59      m = 1;
60
61      %k = 1, then k = 2, k = 3. Loops three times.
62      for k = 1:length(a)
63          %Index n,k in matrix VD and set it to 0.
64          VD(n,k) = 0;
65
66          %Only loops once, length of b is 1.
67          for j = 1:length(b)
```

Figure 6: Snippet of additional comments

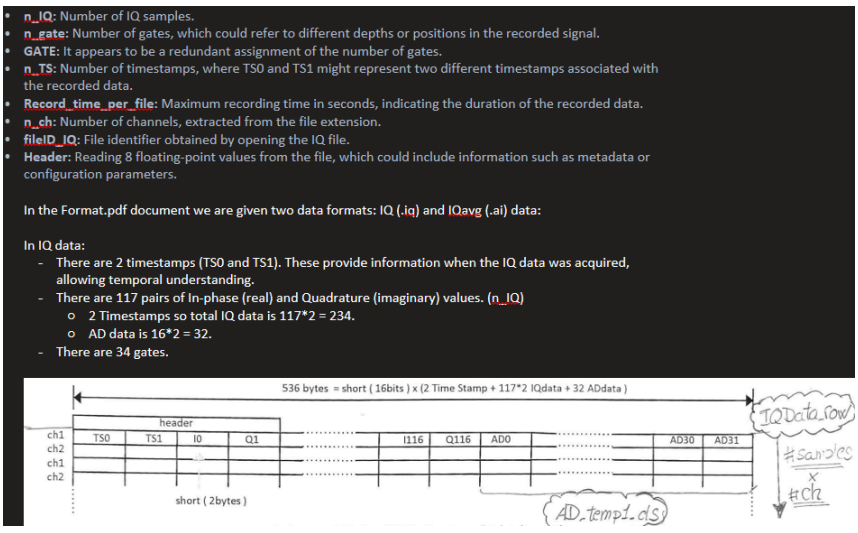

Figure 7: Snippet of data format documentation

Time was given to understanding the context of the raw data format, data flow and parameters involved. The provided format.pdf file was read in detail and made notes on. At a meeting with my supervisor, the data reading process was presented, which encouraged a better understanding of the code and the connection between collection of raw IQ data and how it is used to estimate velocity. Documentation has been made of the parameters in RPData_BrainTV.m, the code used for reading raw avgIQ files.

4. Remaining Work Plan

SDopp implementation and parameters: The SDopp algorithm must be fully commented and understood. Future researchers should easily understand the implementation of the algorithm in reference to the Hoeks et al. (1994) and J. Kucewicz (2004) papers. An indepth documentation must be made.

Code inconsistencies: The MATLAB code must be checked for inconsistencies. For example, an input of the VSDopp function being the period T, which requires the units to be seconds. However, the input used in the code is PRF (Hz). There is no clarity whether this is wrong. Complete knowledge of the BrainTV code is needed.

Mitigation strategies: A significant problem with the current samples, particularly at deeper gates, is the effect of artefacts. Figure 5(a) shows a phase shift that causes extreme superposition. The study by Jiang et al. (2019) [11] reviews ways to remove artefacts. Introducing a method of suppression would be beneficial in reducing the amount of discarded data. Using a supervised learning model will be investigated. Although suppression may be out of scope, having a classification model to identify the errors could be implemented.

5. Support Requirements

- Help understanding the data flow; how to identify the erroneous phase shifts.
- Help understanding the positive echo amplitudes observed in figures 5(c) and 5(d).
- Collaboration with a student/professor knowledgeable on machine learning; insight on how a model in python can be integrated in MATLAB.
- Insight on the methodology involved in the data collection of the IQ samples to help identify reasons for artefacts and noise.
- Insight on the documentation process; how to structure the final report and what subsections to use.
- Feedback and review on the progress; setting tough deadlines weekly to present at meetings.

6. Gantt Chart

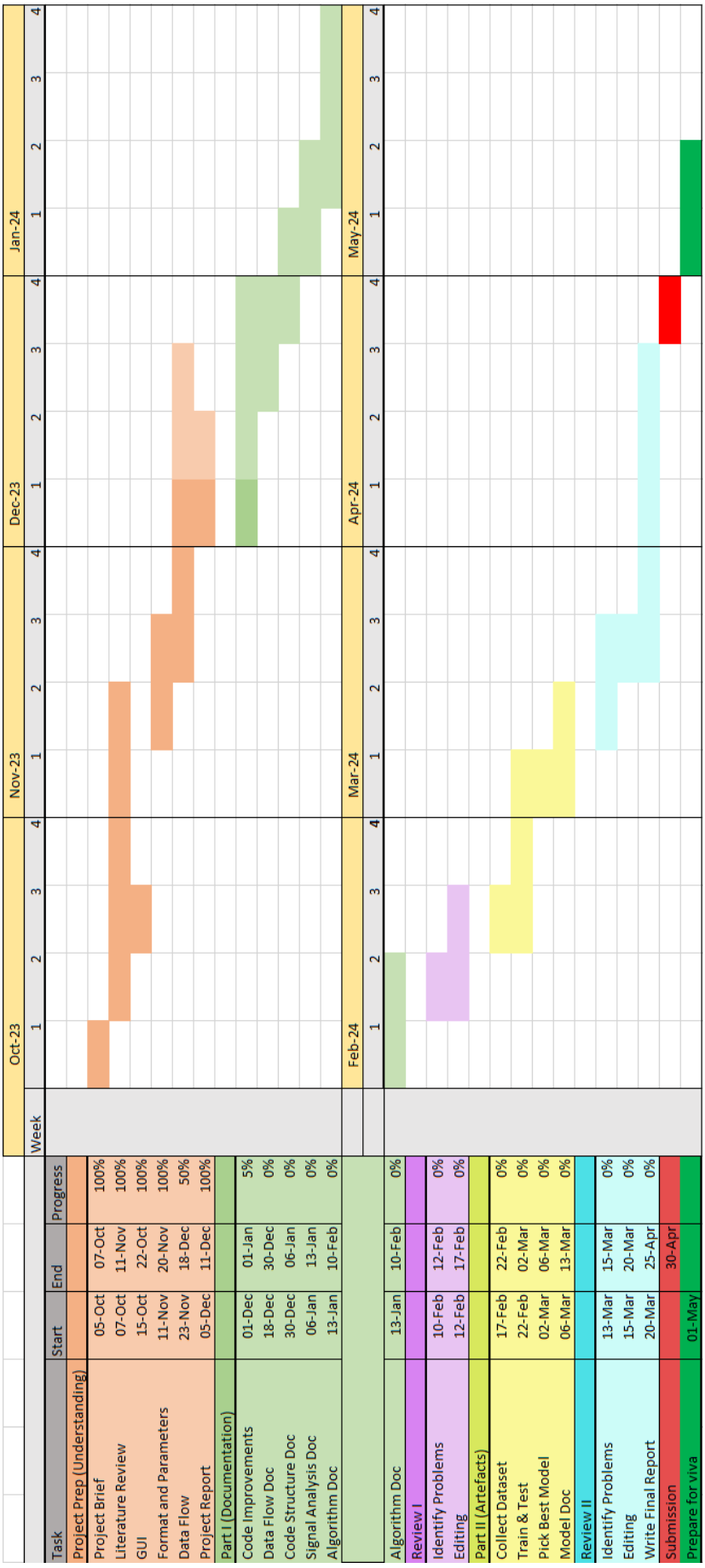

References

[1] A. P. Hoeks, P. J. Brands, T. G. Arts, and R. S. Reneman, "Subsample volume processing of doppler ultrasound signals," *Ultrasound in Medicine Biology*, vol. 20, no. 9, pp. 953–965, 1994. [Online]. Available: https://www.sciencedirect.com/science/article/pii/030156299490054X

[2] A. E. Powles, D. J. Martin, I. T. Wells, and C. R. Goodwin, "Physics of ultrasound," *Anaesthesia Intensive Care Medicine*, vol. 19, no. 4, pp. 202–205, 2018. [Online]. Available: https://www.sciencedirect.com/science/article/pii/S1472029918300171

[3] A. S. Dukhin and P. J. Goetz, "Chapter 3 - fundamentals of acoustics in homogeneous liquids: Longitudinal rheology," in *Characterization of Liquids, Dispersions, Emulsions, and Porous Materials Using Ultrasound (Third Edition)*, third edition ed., A. S. Dukhin and P. J. Goetz, Eds. Elsevier, 2017, pp. 85–118. [Online]. Available: https://www.sciencedirect.com/science/article/pii/B978044463908000003X

[4] M. Ali, D. Magee, and U. Dasgupta, "Signal processing overview of ultrasound systems for medical imaging," *Texas Instruments*, p. 3, 2008. [Online]. Available: https://www.ti.com/lit/wp/sprab12/sprab12.pdf

[5] A. Shah and A. Irshad, *Sonography Doppler Flow Imaging Instrumentation*. Treasure Island (FL): StatPearls Publishing, 2023 May 1. [Online]. Available: https://www.ncbi.nlm.nih.gov/books/NBK580539/

[6] C. Kasai, K. Namekawa, A. Koyano, and R. Omoto, "Real-time two-dimensional blood flow imaging using an autocorrelation technique," *IEEE Transactions on sonics and ultrasonics*, vol. 32, no. 3, pp. 458–464, 1985.

[7] J. C. Kucewicz, "Tissue pulsatility imaging: Ultrasonic measurement of strain due to perfusion," Ph.D. dissertation, University of Washington, 2004.

[8] P. Turner, C. Banahan, M. Alharbi, J. Ince, S. Venturini, S. Berger, I. Bnini, J. Campbell, K. W. Beach, M. Horsfield, M. Oura, A. Lecchini-Visintini, and E. M. Chung, "Brain tissue pulsation in healthy volunteers," *Ultrasound in Medicine Biology*, vol. 46, no. 12, pp. 3268–3278, 2020. [Online]. Available: https://www.sciencedirect.com/science/article/pii/S0301562920303872

[9] D. Zhou, K. F. Cheung, Y. Chen, S. T. Lau, Q. Zhou, K. K. Shung, H. S. Luo, J. Dai, and H. L. W. Chan, "Fabrication and performance of endoscopic ultrasound radial arrays based on pmn-pt single crystal/epoxy 1-3 composite," *IEEE Transactions on Ultrasonics, Ferroelectrics, and Frequency Control*, vol. 58, no. 2, pp. 477–484, 2011.

[10] J. Ince, M. Alharbi, J. S. Minhas, and E. M. Chung, "Ultrasound measurement of brain tissue movement in humans: A systematic review," *Ultrasound*, vol. 28, no. 2, pp. 70–81, 2020. [Online]. Available: https://doi.org/10.1177/1742271X19894601

[11] X. Jiang, G.-B. Bian, and Z. Tian, “Removal of artifacts from eeg signals: A review,” *Sensors*, vol. 19, no. 5, 2019. [Online]. Available: https://www.mdpi.com/1424-8220/19/5/987